

EVALUATION OF ADAPTIVE PARAFAC ALGORITHMS FOR TRACKING OF SIMULATED MOVING BRAIN SOURCES

Ardeshir Fotouhi, Ehsan Eqlimi and Bahador Makkiabadi*, *Member, IEEE*

Abstract— In this paper, we proposed an online 2D localization method for tracking of dynamic moving brain sources. For this purpose, we used an adaptive version of PARAllel FACTor (PARAFAC) analysis for factorization of electroencephalographic (EEG) signals. We utilized Boundary Element Method (BEM) with four layers to solve the forward problem for the simulated EEG signals caused by two moving dipoles within the brain. Then, we created an appropriate tensor built by second order statistics of EEG signals. We adopted an online method to brain source localization called the Recursive Least Squares Tracking (RLST) as an adaptive PARAFAC algorithm with two windowing schemes. Finally, we evaluated the performance of the method applied to EEG signals.

I. INTRODUCTION

EEG is a non-invasive and low cost means to record brain activities and has numerous clinical, psychological and biomedical applications. Usually, existence abnormalities such as seizures and tumor change the intensity and location of activity in specific brain regions. These types of signal variations can be separated and localized, as 2D topoplots on the scalp, by EEG source localization algorithms [1].

A successful EEG source localization process has two most important phases. First, the forward problem which aims to estimate the scalp potentials from the current sources in the brain. Second, the inverse problem which aims to approximation of source locations from scalp potential measurements [2].

The forward problem needs the geometric model of the volume conduction that should be as much as possible close to the human head electrical characteristics. One of the well-known methods called Boundary Element Method (BEM) has been used to implement the forward process with the assumption of having uniform electrical conductivities for three or four layers of brain materials.

The EEG inverse problem is identified as being an ill-posed problem because of having non-unique and unstable solutions. Two types of approaches, such as single dipole and linear distributed current source fitting methods, have been suggested to address this issue and finally providing the 3D location of sources [3].

In the inverse problem, we need to estimate the unknown sources of mixed EEG data and it is similar to the Blind Source Separation (BSS) problem. In the BSS framework, the unknown sources and the mixing matrix will be obtained through the mixture signals. Each row of the mixing matrix

shows the level of closeness of each source signal to different electrodes. With this simple concept, a 2D localization of the sources has been addressed by using topography interpolation algorithms in both online and offline scenarios. Online brain source localization can have beneficial uses in some special areas, such as Brain-Computer Interface (BCI).

Independent Component Analysis (ICA) based methods are more widely used in solving the BSS problem. However, most of the ICA based algorithms require a pre-whitening process as a time consuming process which needs the whole mixture signal is available [4]. Consequently, the majority of ICA algorithms are not suitable for the online applications. In addition, they generally estimate the demixing matrix, as inverse of the mixing system, and therefore the mixing matrix is estimated indirectly [5].

On the other hand, the tensor factorization methodology is a promising and effective technique to tackle the BSS problem by estimating the mixing matrix directly [1]. The tensor factorization algorithms are mostly based on the generalizations of two-way decomposition models to the third-order and higher-order signals. There are several 3-way, or more generally n-way, the factorization algorithms for factorization of the data such as PARAllel FACTor (PARAFAC) analysis.

In the real-time and online the BSS applications the PARAFAC and other tensor factorization methods, in the lack of need to the pre-whitening process, need less computational cost, compared to the ICA based algorithms.

This paper is organized as follows: In Section II, we present the structure of the adaptive PARAFAC algorithm. Section III, discusses about how to generate the tensorial data using the forward model. The experiments and results are provided in Section IV. Finally, the paper is concluded in Section V.

II. ADAPTIVE PARAFAC

The PARAFAC method, also known as Canonical Decomposition (CANDECOMP), is a generalization of a low rank decomposition of matrices to the higher order arrays or the tensors and a powerful multilinear algebra tool. A significant feature of PARAFAC is that its factors are essentially unique under the mild conditions. In this paper, the third-order tensors will be employed.

The PARAFAC [6] decomposes a tensor $\chi \in \mathbb{R}^{I \times J \times K}$ into a sum of R rank-1 tensors, where R represents the smallest number of rank-one tensors as below

$$\chi = \sum_{r=1}^R \mathbf{a}_r \circ \mathbf{b}_r \circ \mathbf{c}_r \quad (1)$$

Where $\mathbf{a}_r, \mathbf{b}_r, \mathbf{c}_r$ are columns of factor matrices $\mathbf{A} \in \mathbb{R}^{I \times R}$, $\mathbf{B} \in \mathbb{R}^{J \times R}$ and $\mathbf{C} \in \mathbb{R}^{K \times R}$, respectively, and \circ denotes the outer vector product. The PARAFAC decomposition can also be expressed in the matrix format. The matrix-wise

A. Fotouhi, E. Eqlimi and B. Makkiabadi* are with the Department of Medical Physics and Biomedical Engineering, School of Medicine, Tehran University of Medical Sciences (TUMS) and Research Center for Biomedical Technologies and Robotics (RCBTR), Institute for Advanced Medical Technologies (IAMT), Tehran, Iran.

*(corresponding author to provide e-mail: b-makkiabadi@tums.ac.ir).

version of (1) could be presented through unfolding the tensor $\mathcal{X} \in \mathbb{R}^{I \times J \times K}$ on possible modes such as $\mathbf{X}^{(1)} \in \mathbb{R}^{IK \times J}$, $\mathbf{X}^{(2)} \in \mathbb{R}^{IJ \times K}$ and $\mathbf{X}^{(3)} \in \mathbb{R}^{JK \times I}$ denoted by $[\mathbf{X}^{(1)}]_{(i-1)K+k,j} = x_{ijk}$, $[\mathbf{X}^{(2)}]_{(j-1)I+i,k} = x_{ijk}$ and $[\mathbf{X}^{(3)}]_{(k-1)J+j,i} = x_{ijk}$, respectively. Where, $[\mathbf{X}]_{i,j}$ denotes the (i,j) th element of the matrix \mathbf{X} .

In order to estimate the PARAFAC factors (\mathbf{A} , \mathbf{B} , \mathbf{C}) the Alternating Least Squares (ALS) is a standard and widely used method. The ALS process leads to perform the following alternating process until convergence:

$$\begin{aligned} \mathbf{B} &= \mathbf{X}^{(1)}((\mathbf{A} \odot \mathbf{C})^T)^\dagger \\ \mathbf{C} &= \mathbf{X}^{(2)}((\mathbf{B} \odot \mathbf{A})^T)^\dagger \\ \mathbf{A} &= \mathbf{X}^{(3)}((\mathbf{C} \odot \mathbf{B})^T)^\dagger \end{aligned} \quad (2)$$

where \odot , $(\cdot)^T$ and $(\cdot)^\dagger$ denote the Khatri-Rao product, the transpose operator and the pseudo-inverse operation, respectively.

The expansion of adaptive algorithms to track the PARAFAC decomposition is an important step towards real-time PARAFAC-based applications. The authors in [7] suggested adaptive PARAFAC algorithm with two types of windowing schemes. In their algorithm, the observed tensor at time $t+1$ being obtained from the old one after appending a new slice along the time dimension and previously calculated factors are used to estimate new ones. This scenario leads to reduce the computational cost compared to the case which applies the standard batch mode PARAFAC repetitively. Therefore, real-time systems with serially acquiring data are potential applications of this method.

The Recursive Least Squares Tracking (RLST) PARAFAC method is developed based on a weighted least-squares recursive algorithm with two exponential and truncated windowing schemes. These windows determine the range of computing so that, with a forgetting factor, all previously observed slices have a different weight to influence the estimated factors. In truncated window scheme, the window has a fixed length that should be larger than the rank of the tensor [7].

Let a third-order tensor $\mathcal{X} \in \mathbb{R}^{I \times J \times K}$, at time t , and considering the Eq. (2) we have,

$$\mathbf{X}^{(1)}(t) \simeq \mathbf{H}(t)\mathbf{B}^T(t) \quad (3)$$

where $\mathbf{H}(t) = \mathbf{A}(t) \odot \mathbf{C}(t)$ has dimensions $IK \times R$, $\mathbf{B}(t) \in \mathbb{R}^{J(t) \times R}$ has a dimension growing with time and $\mathbf{X}^{(1)}(t) \in \mathbb{R}^{IK \times J(t)}$. The main purpose of this algorithm is estimating of recursive updates for $\mathbf{A}(t+1)$, $\mathbf{B}(t+1)$ and $\mathbf{C}(t+1)$ from old estimates $\mathbf{A}(t)$, $\mathbf{B}(t)$ and $\mathbf{C}(t)$. Let $\mathbf{X}(t+1)$ be obtained from $\mathbf{X}^{(1)}(t)$ after appending $\mathbf{x}(t+1)$ (as vectorized representation of the new slice) in the time dimension, such as:

$$\mathbf{X}^{(1)}(t+1) = [\mathbf{X}^{(1)}, \mathbf{x}(t+1)] \quad (4)$$

The overall cost function with exponential windowing (EW) scheme has been considered as follows.

$$\phi^{EW}(t+1) = \sum_{\tau=1}^{t+1} \lambda^{t+1-\tau} \|\mathbf{X}(\tau) - \mathbf{H}(t+1)\mathbf{b}^T(\tau)\|^2 \quad (5)$$

Where λ is the forgetting factor and results the weighted observed matrix by:

$$\mathbf{X}_{EW}(t+1) = \mathbf{X}^{(1)}(t+1)\mathbf{\Lambda}(t+1) \quad (6)$$

Where $\mathbf{\Lambda}(t+1) = \text{diag}([\lambda^{t/2}, \lambda^{t-1/2}, \dots, \lambda^{1/2}, 1])$ is the weighting matrix.

Likewise, we have below definitions for truncated windowing (TW) scheme:

$$\phi^{TW}(t+1) = \sum_{\tau=1}^N \lambda^{N-\tau} \|\mathbf{x}(u+\tau) - \mathbf{H}(t+1)\mathbf{b}^T(u+\tau)\|^2 \quad (7)$$

Where $u = t+1 - N$ that N is the length of window ($N > R$) and $\mathbf{B}_{EW}(t+1)$ consists of the last N rows of $\mathbf{B}(t+1)$.

In the algorithm that uses TW scheme, the weighted observed matrix is defined as:

$$\mathbf{X}_{TW}(t+1) = \mathbf{X}^{(1)}(t+1)\mathbf{\Lambda}(t+1) \quad (8)$$

where $\mathbf{\Lambda}(t+1) = \text{diag}([\lambda^{N-1/2}, \lambda^{N-2/2}, \dots, \lambda^{1/2}, 1])$.

More specifically the RLST-PARAFAC estimates $\mathbf{b}(t+1)$ and consequently $\mathbf{H}(t+1)$ by solving $\nabla\phi(t+1) = 0$ where ∇ is gradient operator (see [7] for more details).

In this paper, we setup a tensor data from stacking the called \mathbf{X}_k . Further description on assumed mixing model for \mathbf{X}_k is provided in the next subsection.

III. GENERATING TENSORIAL DATA USING FORWARD MODEL

In order to evaluate the online localization of moving brain sources, we planned to setup the simulated moving sources within a simulated head model. To this end, we needed to compute the resistive network within the head using the Lead Field Matrix (LFM) that models the relationship between dipole position, the head geometry and the tissue conductivity of the simulated head. The prerequisite for the calculation of the LFM is a head model.

In this paper, we used BEM as a numerical tool to compute the head model parameters to solve the forward problem. Consequently we embedded two moving dipole sources on resulted 3D grid points located on the simulated head model. Then, the generated EEG data after calculating scalp projections of two dipole sources was employed to generate the segmented EEG signals \mathbf{X}_k . All mentioned numerical calculations was done by the freely available Matlab based Neuroelectromagnetic Forward Modeling Toolbox (NFT) [8]. Based on the BSS approach, each \mathbf{X}_k can be decomposed to the mixing (\mathbf{A}) and source matrix (\mathbf{S}_k) as $\mathbf{X}_k = \mathbf{A}\mathbf{S}_k$. Having the independent zero-mean sources results diagonal source covariance matrices \mathbf{D}_k as,

$$\mathbf{D}_k = \mathbf{S}_k\mathbf{S}_k^T \quad (9)$$

Therefore, the mixture covariance matrices can be shown as $\mathbf{R}_k = \mathbf{X}_k\mathbf{X}_k^T = \mathbf{A}\mathbf{D}_k\mathbf{A}^T$ which is one slice of a trilinear tensor \mathbf{R} . Applying the RLST-PARAFAC to the resulted growing trilinear tensor $\mathbf{R} \in \mathbb{C}^{I \times J \times I}$, built by stacking symmetric \mathbf{R}_k matrices, results identical \mathbf{A} , \mathbf{C} matrices (representing the mixing matrix) and \mathbf{B} (which is the result

of stacking diagonal vector of \mathbf{D}_k s and representing the power of sources in each EEG segment) [9].

Moreover, to generate more realistic simulated EEG we have chosen head model with four layers created from T1 weighted Montreal Neurological Institute (MNI) template. Furthermore, 128 electrodes placed on the simulated scalp using standard 10-20 system. The conductivities of different layers were chosen as 0.33, 0.0132, 0.33 and 1.79 (S/m) for the scalp, skull, brain and CSF respectively. Finally, near 50000 grid points with 4 (mm) inter-grid distance were generated by the NFT toolbox.

The simulated Theta (4-8 (Hz)) and Alpha rhythms (8-12 (Hz)) source signals were generated and located on the trajectories passing through sequential 3D gridpoints to produce the EEG scalp potentials.

The dipoles were placed in the left-temporal and central-occipital cortex as the starting points of two trajectories. Then, two dipoles moved over one quarter of the circle inside the brain. Fig. 1 shows one of possible trajectory sets and details of rotational and translational parameters. The trajectories shown in Fig. 1 were chosen due to the fact that Visual Evoked Potentials (VEP) and Steady-State Visually Evoked Potentials (SSVEP) are generally appeared in these areas[10].

Finally, two minutes EEG signal, including two moving brain rhythm sources, were generated with 2000 (Hz) sampling frequency.

In order to take the benefits of RLST tensor factorization algorithm, the 2D simulated EEG must be converted to a third order tensor. In a similar study [11], a time-frequency analysis was applied for creating the tensor from one moving source data, whereas, as we mentioned before, we employed simulated EEG data obtained from two moving sources for creating tensor with space-time-space structure without need of transforming to the frequency domain. For this purpose, as the first step, a temporal EEG segmentation process (e.g. with segment length 340 (ms) and 240 (ms) overlap) has been employed resulting $\chi^{128 \times 500 \times 128}$.

The length of segments and overlap must be chosen with respect to the sampling frequency, maximum frequency of source signals (to achieve the source covariance matrices with less off-diagonal elements), and the minimum time of having quasi-stationary mixing matrix \mathbf{A} . Fig. 2a shows the processes of generation and the factorization of the EEG tensor data.

As it can be seen at Fig. 2b, the new covariance matrix of input EEG signals are entered in an operational window (as a queue of the covariance matrices with the fixed number of

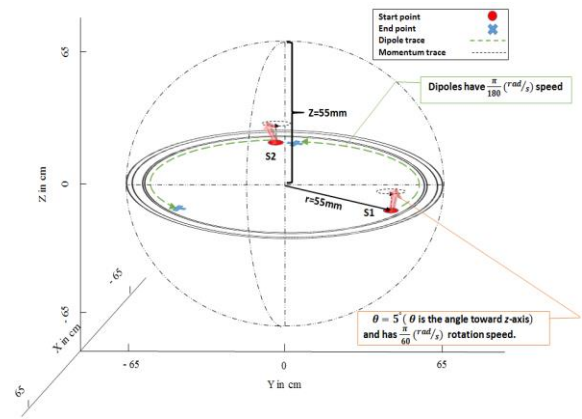


Fig 2. The trajectory of dynamic moving dipoles and their momentums within the 3D head model. Nose is along the positive direction of x-axis

items in the TW scheme and with the whole received items in the EW scheme) for the implementation of the online brain source localization algorithm. In the EW scheme, the weights are set such that the new data have the greatest impact in the cost function ϕ^{EW} whereas in TW scheme has a fixed size operational window such that the new covariance matrix is added after removing the oldest matrix

(see Fig.2b). The forgetting factor in both operational windows was chosen as $\lambda = 0.85$.

The topoplots related to the columns of \mathbf{A} (estimated by applying the online RLST tensor factorization algorithm at each step) shows the approximation of both source locations in 2D scalp map. Fig. 3 shows the original and the estimated location (by EW and TW schemes) of two sources along time (see Fig. 3).

IV. EXPERIMENTAL RESULTS

In order to evaluate the performance of RLST based algorithms and for comparing two operational windowing schemes on brain source localization, we employed four metrics i.e. Channel Error (CE), 2D Error (2DE), Peak Signal-To-Noise Ratio (PSNR), and Normalized 2D Correlation Coefficient (N2DCC). These metrics were calculated for the results of several experiments on simulated EEG data built by different scalp projections that obtained by placing and moving two dipoles from the different starting points and different depths within the head model. Furthermore, in order to evaluate the robustness of

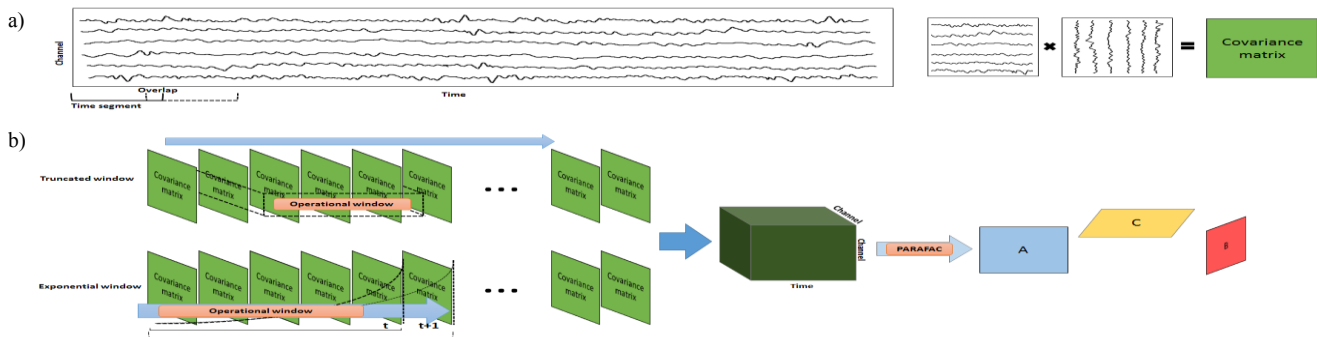


Fig 1. Schematically show how to generate three dimensional EEG data a) Concept of temporal segmentation, overlap and covariance matrix and b) Concept of adaptive PARAFAC with truncated and exponential window

the algorithms to the additive Gaussian noise, each experiment has been done in the presence of the different noise levels (using simulated EEGs with different Signal-to-Noise Ratio (SNR) levels).

Fig. 3 shows the topographic results of one of the experiments that its EEG dipole source trajectories were shown at Fig. 1. Moreover, Table I shows averaged metrics of 10 different trajectories with 5 different randomly generated sources at three SNR levels (0dB-10dB-20dB).

The overall results in Table I show that the TW scheme has shown better performance compared to the EW one. In addition, because of utilizing the second order statistics (covariance matrices) of EEG signals the whole localization algorithm is expected to be more robust against additive noise compared to the methods of dealing with EEG signals directly. Expectedly, the results of the experiments confirm this concept especially for the cases with SNR levels of 10dB and 20dB. Also, it can be seen that even on the very noisy cases with 0dB SNR the metrics are still promising.

V. CONCLUSIONS

In this paper, we utilized an adaptive PARAFAC algorithm, with two operational windowing schemes, for localizing and tracking of dynamic EEG sources on 2D map of the scalp. To this end, we placed the sources on the grid points of a simulated head model, estimated from real MR images, and moved them through a predefined trajectory to create the related 128-channel EEG signal.

Then, we used temporally segmented EEG signals to compute their covariance matrices and consequently build up the tensor data. In the next step, the RLST based PARAFAC algorithm was applied to the growing tensor and the estimated factor A , after adding each new arriving covariance matrix, was reported as the mixing channel to localize the simulated sources online. The estimated tracks of sources were compared to the original ones by measuring four metrics i.e. channel error, 2D error, 2D PSNR, and normalized 2D correlation coefficient. Promising results achieved in tracking of the simulated moving sources with different trajectories and in the presence of different level of added noise.

In addition, we compared performance of both TW and EW windowing schemes and the TW scheme, with lower computational cost, showed better performance. As another striking feature of the proposed algorithm is noise-robustness due to employing second order statistic. Further experiments and results over the real EEG signals also evaluating and comparing our results with the well-known online-ICA algorithms is under progress and will be reported in future publications.

TABLE I. THE NUMERICAL RESULTS FOR TWO WINDOWING SCHEME IN TERMS OF CHANNEL ERROR(CE), 2D ERROR(2DE), PSNR AND NORMALIZED 2D CORRELATION COEFFICIENT(N2DCC)

Window	Exponential			Truncated		
	0dB	10dB	20dB	0dB	10dB	20dB
CE	-24.486	-39.671	-40.199	-30.848	-41.666	-42.071
2DE	-33.958	-47.091	-47.648	-39.146	-48.812	-49.291
PSNR	30.289	35.694	36.330	32.050	36.343	36.939
N2DCC	0.905	0.984	0.985	0.944	0.987	0.988

ACKNOWLEDGMENT

This study was part of a M.S. thesis supported by Tehran University of Medical Sciences; Grant no. 93-02-30-26138.

REFERENCES

- [1] B. M. Abadi, D. Jarchi, and S. Sanei, "Simultaneous localization and separation of biomedical signals by tensor factorization," in *Statistical Signal Processing, 2009. SSP '09. IEEE/SP 15th Workshop on*, 2009, pp. 497-500.
- [2] H. Hallez, A. Vergult, R. Phlypo, P. Van Hese, W. De Clercq, Y. D'Asseler, et al., "Muscle and eye movement artifact removal prior to EEG source localization," in *Engineering in Medicine and Biology Society, 2006. EMBS '06. 28th Annual International Conference of the IEEE*, 2006, pp. 1002-1005.
- [3] J. Daunizeau, J. Mattout, D. Clonda, B. Goulard, H. Benali, and J. M. Lina, "Bayesian spatio-temporal approach for EEG source reconstruction:conciliating ECD and distributed models," *Biomedical Engineering,IEEE Transactions on*, vol. 53, pp. 503-516, 2006.
- [4] G. R. Naik and D. K. Kumar, "An overview of independent component analysis and its applications," *Informatica:An International Journal of Computing and Informatics*, vol. 35, pp. 63-81, 2011.
- [5] H. Wei-Chung, H. Shao-Hang, C. Jen-Feng, C. Meng-Hsiu, V. Lan-Da, and L. Chin-Teng, "FPGA implementation of 4-channel ICA for on-line EEG signal separation," in *Biomedical Circuits and Systems Conf, 2008.BioCAS 2008.IEEE, 2008*, pp.65-68.
- [6] A. Smilde, R. Bro, and P. Geladi, *Multi-way analysis: applications in the chemical sciences*: John Wiley & Sons, 2005.
- [7] D. Nion and N. D. Sidiropoulos, "Adaptive Algorithms to Track the PARAFAC Decomposition of a Third-Order Tensor," *Signal Processing,IEEE Transactions on*, vol. 57, pp. 2299-2310, 2009.
- [8] Z. A. Acar and S. Makeig, "Neuroelectromagnetic Forward Head Modeling Toolbox," *Journal of Neuroscience Methods*, vol. 190, pp. 258-270, 7/15/ 2010.
- [9] B. Makkiabadi and S. Sanei, "Factorization based blind identification and separation of nonstationary seizure signals," in *Artificial Intelligence and Signal Processing (AISP), 2012 16th CSI International Symposium on*, 2012, pp. 617-622.
- [10] F.-B. Vialatte, M. Maurice, J. Dauwels, and A. Cichocki, "Steady-state visually evoked potentials: Focus on essential paradigms and future perspectives," *Progress in Neurobiology*, vol. 90, pp. 418-438, 4/ 2010.
- [11] J. Mengelkamp, M. Weis, and P. Husar, "Evaluation of multi-dimensional decomposition models using synthetic moving EEG potentials," in *Signal Processing Conference (EUSIPCO), 2013 Proceedings of the 21st European*, 2013, pp. 1-5.

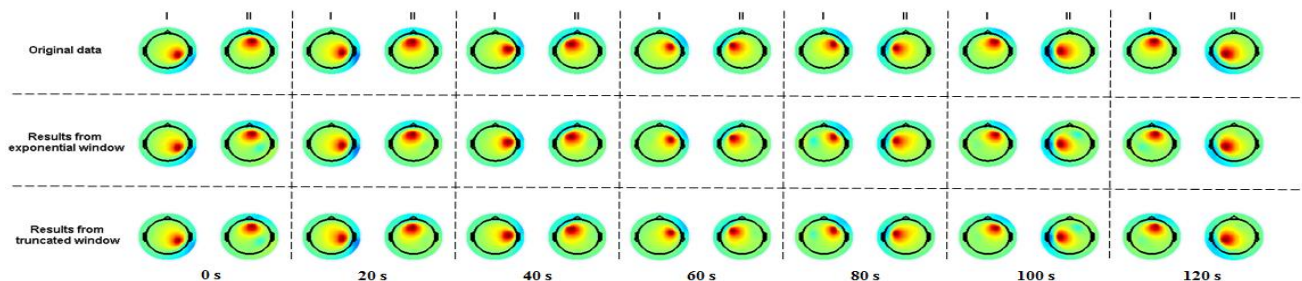


Fig 3. Comparison of topographic maps between original simulated data and results of RLST algorithm